



1D Tensile Damage Propagation Modeling by Two Scale Approach

Oumar KEITA^{1*}, Bertrand FRANCOIS²

¹Université de N'Zérékoré, Département d'Hydrologie, N'Zérékoré, Guinée.

²University of Liège Geotechnical engineering Urban and Environmental Engineering Faculty of Applied Sciences, Liege, Belgium

Abstract: Dynamic damage phenomenon of quasi-brittle materials is often better addressed by micromechanical tensile modeling. The macroscopic dynamic damage evolution is due to micro-crack propagation. One of the ways to address this issue is the analysis of micro-structural damage process. This paper presents a 1D tensile damage model using two scale approach. The dynamic damage law is implemented in a finite elements code to simulate the macroscopic behavior of 1D tensile dynamic damage propagation. The dependency of the structural response on microstructural size and the initial damage value is illustrated

Keywords: Tensile, Damage, 1Dimension, Two scale, Modeling, propagation

1. Introduction/ Background

When materials are subjected to high and rapid changes of stresses (due to dynamic loading) the damage process is governed by dynamic behaviour of fractures. The description of the damage evolution process under dynamic loading of quasi-brittle materials is currently a real scientific challenge [1].

Generally, two approaches are often used to model the dynamic damage phenomenon: the phenomenological approach and the micromechanical one. Although some micromechanical models in compression have been developed ([2],[3]), micromechanical tensile models seem to better reproduce the phenomenon of dynamic damage.

Dynamic crack propagation and branching is studied with a new rate-dependent stress-based nonlocal damage mode in [4]. Dynamic propagation of a macrocrack interacting with parallel small cracks is studied in [5]. Simulation of the tensile damage and blast crater near free face of rock massis performed in [6]. Numerical prediction of dynamic tensile failure in concrete by a corrected strain-rate dependent nonlocal material model is investigated in [7].

Despite the existence of these numerous models of damage and fragmentation of tensile rock, few multiscale models exist for the tensile damage among which we can cite ([8], [9] and [10]). Dynamic rock tensile phenomena are often illustrated using Hopkinson bar tests ([11], [12] and [13]).

One of the ways to address this issue is the analysis of micro-structural damage process. The macroscopic damage evolution is due to micro-crack propagation. For this purpose, we use the recent dynamic damage model accounting for inertial effects deduced from a two-scale framework analysis developed by [1], [14]. The model is implemented in LAGAMINE finite element code to simulate the macroscopic behavior of uniaxial tensile Damage response. This paper is structured as following. After the introduction section above, the dynamic damage model is first presented. Tensile damage propagation simulation is the presented. Then a parametric study is performed to highlight in influence of the microstructural length on dynamic damage response.



All content should be written in English and should be in Single column.

2. Materials and Methods

Dynamic damage model

In [1] and [14], the dynamic Equations of the present damage model were established. Based on the asymptotic homogenization schemes and damage evolution from energy release rate analysis the following set of dynamic Equations was found

The momentum balance Equation is

$$\frac{\partial \Sigma_{ij}^{(0)}}{\partial x_j} = \langle \rho \rangle \frac{\partial^2 u_1^{(0)}}{\partial t^2} \tag{1}$$

The macroscopic stress expression is

$$\Sigma_{ij}^{(0)} = C_{ij11}(d) e_{x11}(u^{(0)}) \tag{2}$$

Where $C_{ij11}(d)$ is the damaged stiffness tensor defined as:

are the homogenized coefficients, in which ξ^{kl} represents the unit cell mode deformation ([15] and [16]). From the above Equations (1-2), the dynamic damage evolution law for vertical and horizontal micro-cracks orientation is (see [1] for more details)

$$\frac{dd}{dt} = \frac{2C_R}{\varepsilon} \left(\frac{G_c}{\varepsilon \frac{\partial C_{ijkl}(d)}{\partial d} e_{xkl}(u^{(0)}) e_{xij}(u^{(0)})} + \frac{1}{2} \right) \tag{3}$$

Where C_R is the Rayleigh wave speed, ε materials microstructural length, G_c the critical energy release rate. For the material with elastic parameters $E=2$ GPa and $\nu=0.3$, the computed homogenization coefficients are represented in the following Figure 1.

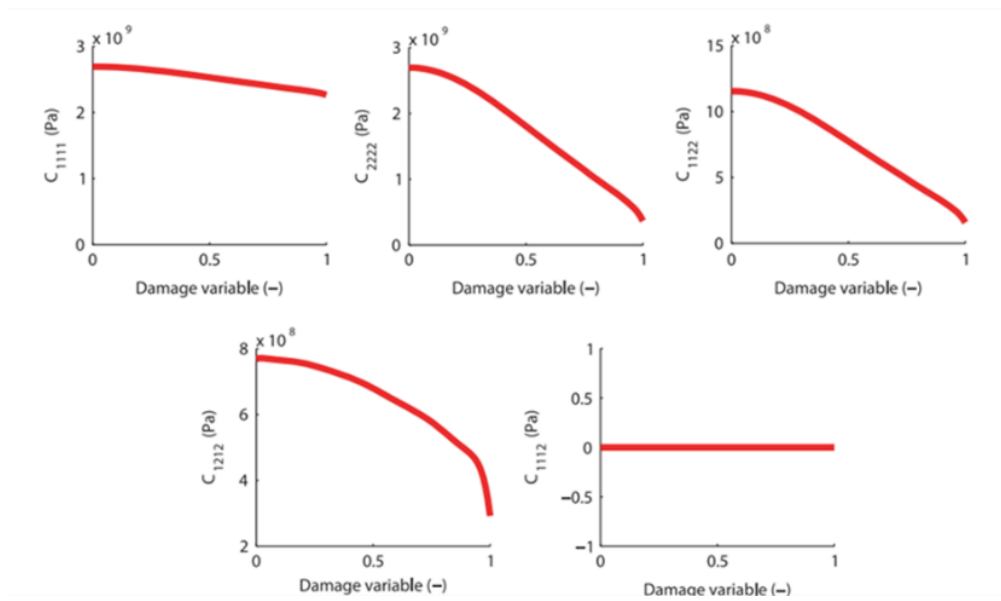


Figure 1: Homogenized coefficients for elastic parameters $E=2$ GPa and $\nu=0.3$ in vertical crack opening

1D Tensile Damage Propagation Simulation

In this section the dynamic damage evolution law (Equation 3) is applied to a specimen with a vertical orientation of micro-cracks submitted under uniaxial tensile load to simulate 1D damage propagation.

Loading

The following explosion pressure time history has been considered

$$P = P_d \left(\frac{d_c}{d_h} \right)^3 \frac{t}{t_r} e^{\left(1 - \frac{t}{t_r} \right)} \tag{4}$$

Where d_c , and d_h are the diameters of the explosive and blasthole (mm), respectively. P_d is the detonation



pressure (Pa) which is the pressure exerted by the expansion of gases from the explosion. It can be calculated from the following Equation as suggested by the National Highway Institute [17]:

$$P_d = \frac{449.93 \times SG_e \times VOD^2}{1 + 0.0855 SG_e} \tag{5}$$

Where, SG_e is the density of the explosive (g/cm^3), VOD is the detonation velocity of the explosive (m/s), t is the elapsed time, and t_r ($= 0.0003361$ s) is the time to reach peak pressure. The value of P_d , d_c and d_h are determined according to the type of explosive. In this study we consider the explosive. Emulstar 3000 UG (see table.1)

Table 1: characteristic of EMULSTAR 3000 UG

SG_e (kg/m3)	VOD (m/s)	P_d (GPa)	d_c (mm)	d_h (mm)	t_r (s)
1.25	5600	9.9	80	165	0.0003361

Geometrical Modeling

The schematic representation of the uniaxial tensile test is shown in Figure 2

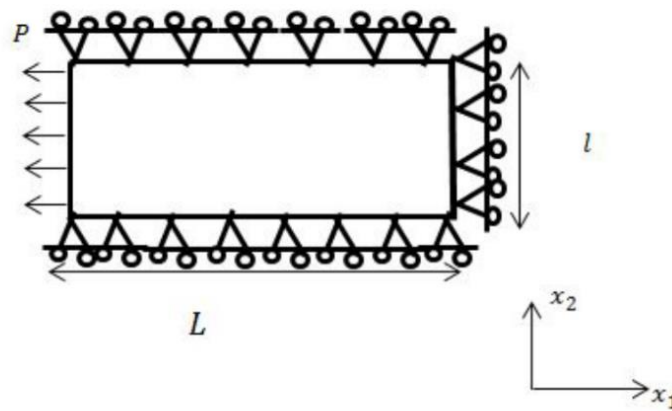


Figure 2: Geometry and loading for a uniaxial tensile test

3. Results & Discussion

In this section the results of damage variable evolution, the uniaxial stress and strain during damage propagation. The parametrical study is carried out to determine the influence of the microstructural length and initial damage value on damage propagation and stress-strain behavior.

Case of zero damage, comparison with the elastic case

In this sub-section we performed some simulations by considering in our dynamic damage law a zero initial damage value in order to compare the results to those of a pure elastic law. For an initial damage value $d_0=0$ and by imposing a zero variation of damage $dd/dt= 0$, the material behavior should be the same as for a elastic law, this is confirmed by the figure 3. Figure 3 gives the comparison between the damage law for $d_0=0$ and a elastic law for the same material (Figure 3.a, b) and uniaxial stress profile at different time (Figure 3. c, d). We can clearly see that the uniaxial stress state σ_{xx} and profile are the same in the two simulations. Which validates the stress-strain integration of our damage law in the finite elements code used.

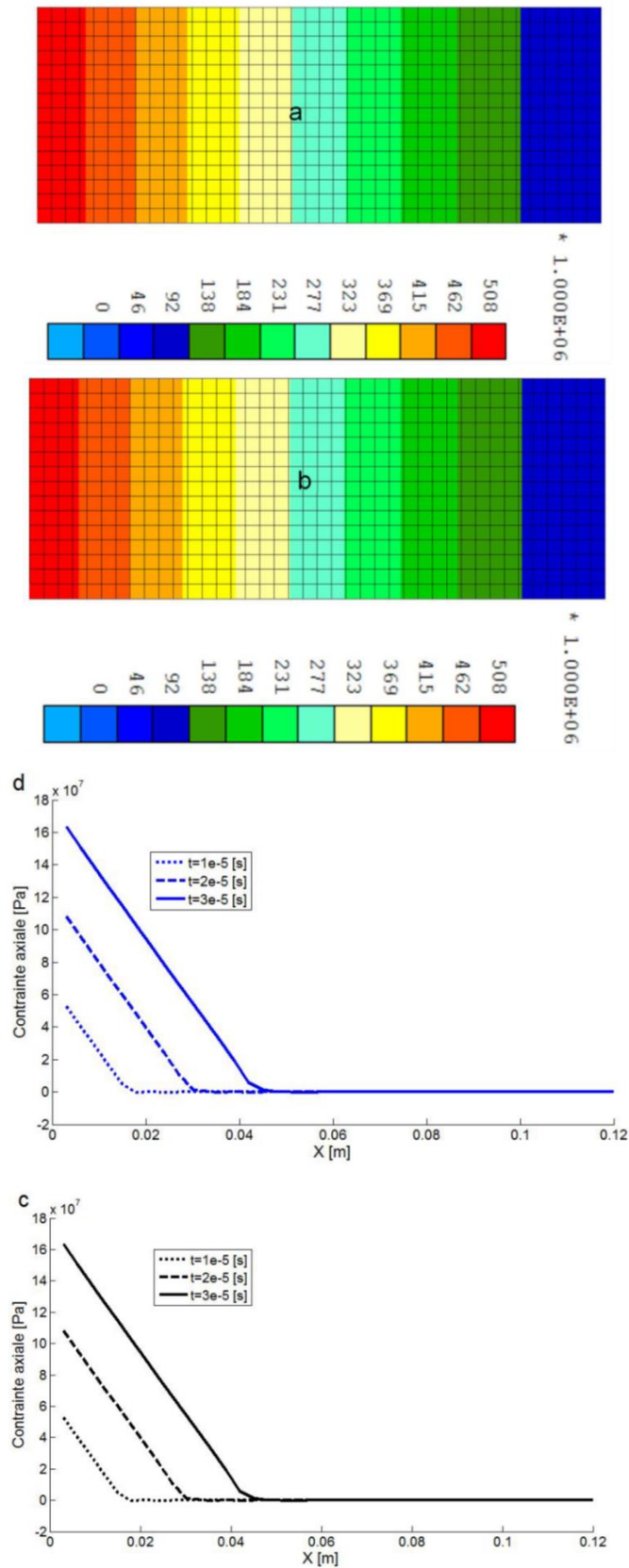


Figure 3: Axial component of the stress state σ_{xx} evolution until time $t=1.007 \times 10^{-4}$ s: a) elastic law, b) dynamic damage law for $d_0=0$. Axial stress profile at different time: c) elastic law, d) dynamic damage law for $d_0=0$



Parametric study of damage evolution and stress-strain behavior

In this test the damage is obtained using homogenized coefficients in the microscopic problem whose cracks are vertical orientation. The initial damage value is $d_0=0.2$. Figure 4 illustrates damage evolution at different loading time.

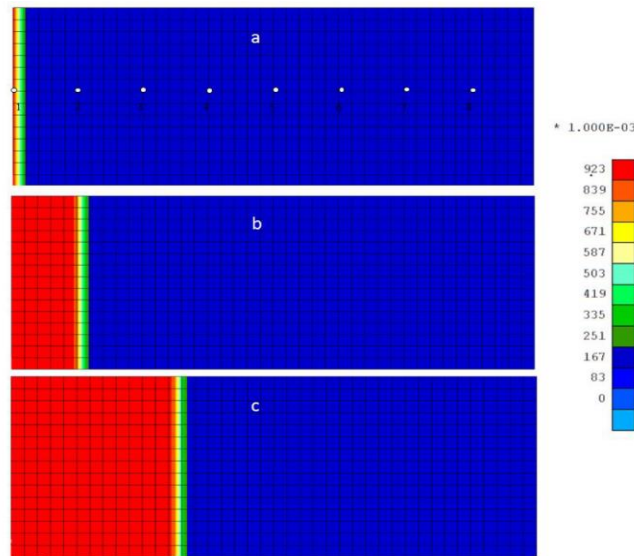


Figure 4: Damage zone evolution for different dynamic loading times

We remark the damage front increases with loading duration. Figure 5 shows the global macroscopic behavior at time $t=9.44 \times 10^{-6}$ s at point 1 (see point 1 on Figure 4 a). We observed the results is the same as the microscopic behavior in [1]. At the start of loading, the stress-strain relation is linear because the damage does not evolve. When the deformation generates an increase in damage, the behavior softens revealing a peak in the stress-strain relation. Finally at $d=1$ (full damage), there remains residual rigidity

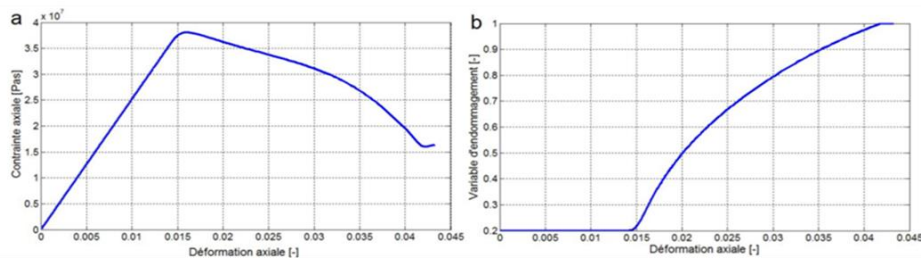


Figure 5: Global macroscopic behavior evolution until time $t=9.44 \times 10^{-6}$ s: a) of axial stress, b) of Damage variable in function of axial strain at point 1 (Figure 4 a).

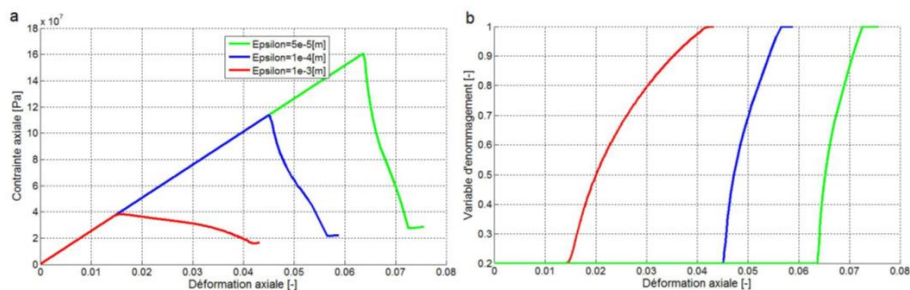


Figure 6: Influence of microstructural lengths, global macroscopic behavior curves evolution until $t=9.44 \times 10^{-6}$ s: a) of axial stress, b) of damage variable in function of axial strain for different values of ϵ (microstructural length).

Then, we analysis the influence of the microstructural length on the structural response of materials. In Figure 6 we present the stress-strain and damage-strain curves for three simulations with different microstructural lengths. We note that for small sizes of the microstructure, we obtain the rupture of the material with very high stresses. In other words, the smaller the microstructure size is, the more resistant the material is to damage, and the behavior becomes more fragile (Figure 6.a). The material behavior is also ductile when the microstructural length is high. This is explained by the fact that the cracks must propagate over a large distance before completely cracking the cell.

Let's now analyze the evolution of the damage outside and inside the damaged zone. Figure 7 shows the position of the three zones at different distance from the left end of the specimen where the dynamic load is applied and the corresponding damage variable distribution, d at time $t=1.0 \cdot 10^{-5}$ s. We see that damage increases from zone 1 to zones 2 and 3 (Figure 7 a). At the level of zone 3, the damage does not evolve, because it is not yet affected by the dynamic wave at the time $t=1.0 \cdot 10^{-5}$ s.

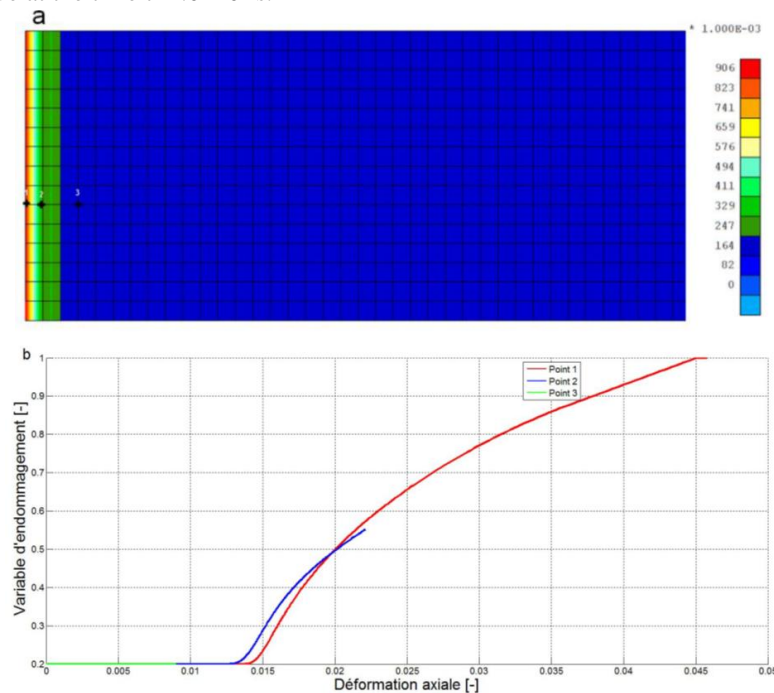


Figure 7: Damage evolution for different elements located outside and in the damage zone until time $t=1.0 \cdot 10^{-5}$ s: a) damage zones with elements, b) damage variable evolution d , at point 1, 2 and 3

Finally, we show the sensitivity of the damage evolution to the initial damage value d_0 . Figure 8 represents the stress-strain and damage-strain curves for three simulations with different initial damage value d_0 . They correspond to the initiation with pre-existing micro-cracks of different lengths ($d_0 = 0$, $d_0 = 0.2$ and $d_0 = 0.5$ respectively)

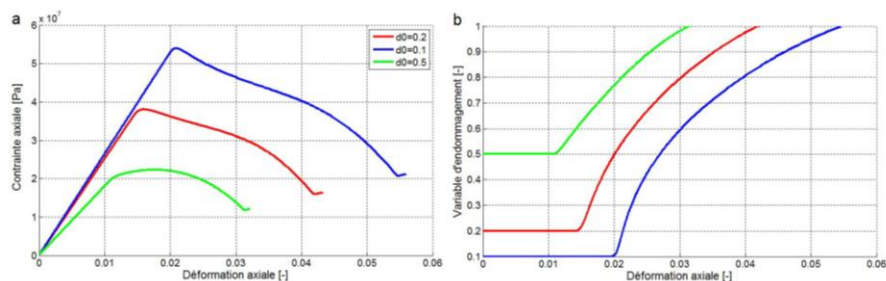


Figure 8: Influence of initial damage d_0 , global macroscopic behavior curves evolution until $t=9.9 \cdot 10^{-6}$ s: a) of axial stress, b) of damage variable in function of axial strain at point 1 (Figure 4 a) for different initial damage values d_0 .

We observed for high initial damage values d_0 , damage evolves more rapidly leading to a lower material resistance stress value, while for small values of the initial damage d_0 , the material is difficult to damage because it is more resistant (Figure 8 a,b). This fact is also illustrated in Figure 9 by the iso-values map of damage variable, which shows that the smaller the initial damage value d_0 is, the smaller the damage zone is, because the material is more resistant

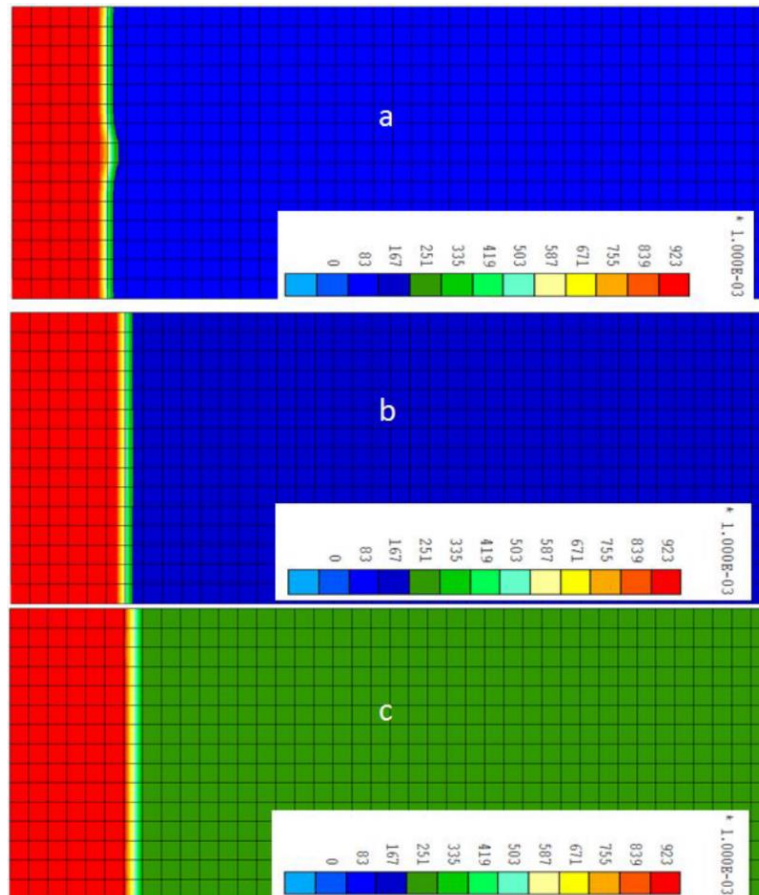


Figure 9: Influence of initial damage d_0 on damage zone at time $t=1.0 \cdot 10^{-5}$ s: a) $d_0=0.1$, b) $d_0=0.2$, c) $d_0=0.3$

4. Conclusion

This paper allowed simulating the 1D tensile dynamic damage propagation. The new dynamic damage law account inertial effect was implemented in a finite elements code to study the global behavior of dynamic damage.

To show the model capability, first, we performed some simulations by considering in our dynamic damage law a zero initial damage value in order to compare the results to those of a pure elastic law. For an initial damage value $d_0=0$ and by imposing a zero variation of damage $dd/dt=0$, we found the material behavior is the same as for a elastic law. Then the dynamic damage propagation was simulated and the macroscopic behaviors: stress-strain and damage-strain were computed. Finally the parametric study were performed to illustrate the influence of materials microstructural length and the initial damage value on damage response. It was shown for small sizes of the microstructure, we obtain the rupture of the material with very high stresses. In other words, the smaller the microstructure size is, the more resistant the material is to damage, and the behavior becomes more fragile. We observed for high initial damage values d_0 , damage evolves more rapidly leading to a lower material resistance stress value, while for small values of the initial damage d_0 , the material is difficult to damage because it is more resistant



References

- [1]. Keita O, Dascalu C, François B. A two-scale model for dynamic damage evolution. *J. Mech. Phys. Solids*. 2014; 170 -183.
- [2]. Nemat-Nasser S, Deng H (1994) Strain-rate effect on brittle failure in compression. *Acta Metall Mater* 42:1013-1024
- [3]. Chengyi, Ghatu Subhash, Stanley J. Vitton (2002). A dynamic damage growth model for uniaxial Compressive response of rock aggregates, *Mechanics of Materials*, Volume 34, Issue 5, 2002, Pages 267-277.
- [4]. L. Pereira, J. Wertheim and L.J. Sluys (2016). Simulation of dynamic behavior of quasi-brittle materials with new rate dependent damage model. 9th International Conference on Fracture Mechanics of Concrete and Concrete Structures.
- [5]. Bozo Vazic, Hanlin Wang, Cagan Diyaroglu, Selda Oterkus, and Erkan Oterkus (2016). Dynamic propagation of a macrocrack interacting with parallel small cracks. *AIMS Materials Science*, 4(1): 118-136. DOI: 10.3934/matserci.2017.1.118.
- [6]. Zhiliang Wang, Yongchi Li, J.G. Wang, A method for evaluating dynamic tensile damage of rock, *Engineering Fracture Mechanics*, Volume 75, Issue 10, 2008,
- [7]. Xiangzhen Kong, Qin Fang, Jinhua Zhang, Yadong Zhang, Numerical prediction of dynamic tensile failure in concrete by a corrected strain-rate dependent nonlocal material model, *International Journal of Impact Engineering*, Volume 137, 2020, 103445
- [8]. Li XF, Zhang QB, Li HB, Zhao J (2018) Grain-based discrete element method (GB-DEM) modelling of multi-scale fracturing in rocks under dynamic loading. *Rock Mech Rock Eng* 51:3785–3817
- [9]. Fuxin R, Gao-Feng Z, Yuliang Z, Lifeng F, Xiaobao Z (2023) Study on the Mechanism of Rock Damage Under Microwave and Laser Irradiation Through Multiscale and Multiphysics Numerical Modelling. *Rock Mech Rock Eng* <https://doi.org/10.1007/s00603-023-03608-5>
- [10]. Zhao GF, Zhang Y, Hou S et al (2022) Experimental and Numerical Studies on Small-Scale Direct Tension Test for Rock. *Rock Mech Rock Eng* 55 669–690 <https://doi.org/10.1007/s00603-021-02683-w>
- [11]. Xia KW, Yao W (2015) Dynamic rock tests using split Hopkinson (Kolsky) bar system-a review. *J Rock Mech Geotech* 7:27–59
- [12]. Xie H, Zhu J, Zhou T et al (2021) Novel Three-dimensional Rock Dynamic Tests Using the True Triaxial Electromagnetic Hopkinson Bar System. *Rock Mech Rock Eng* 54, 2079–2086
- [13]. Li C, Kang L, Qi Q, et al (2009) The numerical analysis of borehole blasting and application in coal mine roof-weaken. *Procedia Earth and Planetary Sciences*
- [14]. Keita O, François B (2015) A microstructurally-based internal length for strain localization problems in dynamics. *European Journal of Mechanics A/Solids* 53 (2015) 282-293.
- [15]. Dascalu, C., Bilbie, G., Agiasofitou, E., 2008. Damage and size effect in elastic solids: a homogenization approach. *Int. J. Solid Struct.* 45, 409–430.
- [16]. François, B., Dascalu, C., 2010. A two-scale time-dependent damage model based on non-planar growth of micro-cracks. *J. Mech. Phys. Solids* 58 (11), 1928-1946
- [17]. Konya, CJ, Walter, EJ, 1991, Rock blasting and overbreak control. FHWA-HI-92-001, National Highway Institute, 5 pp

